# General method for the synthesis of crystalline organic nanorods using porous alumina templates

**Rabih O. Al-Kaysi and Christopher J. Bardeen***

*Received (in Berkeley, CA, USA) 25th November 2005, Accepted 20th January 2006*
*First published as an Advance Article on the web 2nd February 2006*
**DOI: 10.1039/b516732a**

**Nanorods composed of a variety of conjugated organic molecules were synthesized using an anodized alumina template and solvent annealing; detailed study of 200 nm thick 2,7-di-*t*-butylpyrene rods showed they are crystalline, with single domains extending over several microns.**

Nanoscale aggregates of conjugated organic molecules can exhibit properties useful in applications like solar energy conversion[1] and fluorescence sensing.[2] The synthesis of such organic nanostructures with good control over both size and morphology is challenging because the cohesive forces between units (molecules) are relatively weak compared to the covalent bonds found in inorganic materials. Hence preparations based on uncontrolled assembly, like reprecipitation,[3] tend to result in a wide distribution of particle sizes, although varying conditions like temperature or concentration can afford some control over the mean particle size.[4–6] A more promising route is the use of uniformly sized templates which force the organics to assemble within a well-defined space. The commercial availability of high porosity $Al_2O_3$ filters has made them the most commonly used template for the fabrication of organic nanotubes and nanowires.[7–14] Because of the surface energy gained by interaction of the organics with the walls of the $Al_2O_3$ channels, the most common outcome of exposing such membranes to organics is the formation of tubes.[15,16] Often, the internal structure and crystallinity of nanorods grown by the template method are unclear. Other methods have been used to grow crystalline rods, for example by using a crystalline surface[17–19] or solid phase thermal reactions,[20] but at the expense of size control. This variation in outcomes, along with the sometimes extreme (high temperature) conditions used in some methods, demonstrates the need for a general method for preparing solid, preferably crystalline, organic nanorods.

In this Communication, we present such a method. By using a combination of solvent saturation and low temperature solvent annealing, we show that 200 nm diameter organic nanorods can be fabricated using a variety of conjugated organic molecules. A detailed investigation of rods of 2,7-di-*t*-butylpyrene (DTBP)[21] shows that these rods are solid and composed of large single crystalline domains which extend over several microns or more. Preliminary work shows that the mechanism of their formation likely involves the simultaneous formation of many crystallites within the channel, which then eventually fuse into a single, larger crystalline domain. The method presented here should be general enough and sufficiently mild to allow the investigation of size-dependent effects in many different types of organic molecular crystals.

The general method for preparing organic nanorods is as follows: A solution of the organic material in tetrahydrofuran (THF) usually between 0.1 and 0.07 M was deposited over commercially available alumina Anodisc filters (Whatman Ltd., Anodisc 13) with a 200 nm quoted diameter. The organic solution was gradually added *via* pipet ($\sim$ 0.15 ml) to both faces of the Anodisc and air dried. The disk surface was manually polished using 1500 grit sandpaper to remove excess organic material. The same process was repeated several times. Finally the polished alumina Anodisc was placed in a commercially available plastic filter holder (Structure Probe, Inc.) which contacted only its polypropylene ring. The assembly was placed inside a 150 mL capacity jar padded with cotton and soaked with 15 ml of THF. The jar was tightly sealed by capping it with polyethylene film then aluminium foil and sealing the sides with Teflon tape. The jar was then placed inside an oven set at 67–70 °C for a period of 24 hours. The jar was removed and allowed to gradually cool to room temperature before opening. At this time all the THF solvent had evaporated. Finally the Anodisc is given a quick polish with the 1500 grit sandpaper and the alumina template dissolved away using 2 M aqueous potassium hydroxide solution. The organic nanorods were filtered on top of a 0.8 μm cellulose filter and washed with deionized water. The nanorod yield was estimated using a fluorescence microscope to examine the relative amounts of rods *versus* other types of fluorescent aggregates. For DTBP, only fluorescent bundles of nanorods were visible. In contrast, annealing the loaded alumina Anodisc using heat only (70 °C) for 24 hours, without solvent, yielded only a random fluorescent powder. A drop of the water suspension of organic nanorods was placed on Cu tape, dried and sputtered with Au/Pt for the scanning electron microscopy (SEM) experiments. For the transmission electron microscopy (TEM) measurements, the rods in aqueous solution were deposited on top of a 2 nm thick graphite membrane.

Figs. 1a and b show SEM images of the DTBP rods after dissolving away the Anodisc membrane. Unlike hollow tubes, the ends of the rods are flat and uniform, without the fluted appearance often seen in the ends of tubes (see Fig. 5d). Furthermore, these structures are very robust under electron bombardment. No swelling or bending was observed; instead, the rods fracture perpendicular to their long axis, resulting in shorter rods. The robust nature of the rods is likely the result of their crystallinity. Fig. 2 shows a TEM darkfield image of two $\sim$ 5 micron long rod segments lying side by side on a graphite membrane.

*Department of Chemistry, University of California, Riverside, CA, USA. E-mail: christob@ucr.edu; Fax: (951) 827-4713; Tel: (951) 827-2723*

 

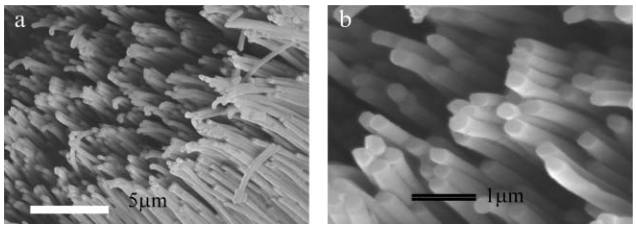


**Fig. 1** a) FESEM image of DTBP nanorods fixed on Cu tape with the alumina support completely etched out. b) Close up lateral view of DTBP nanorods. Rod diameter ~ 210 nm. Some nanorods are 50 microns long (the thickness of the Anodisc template).

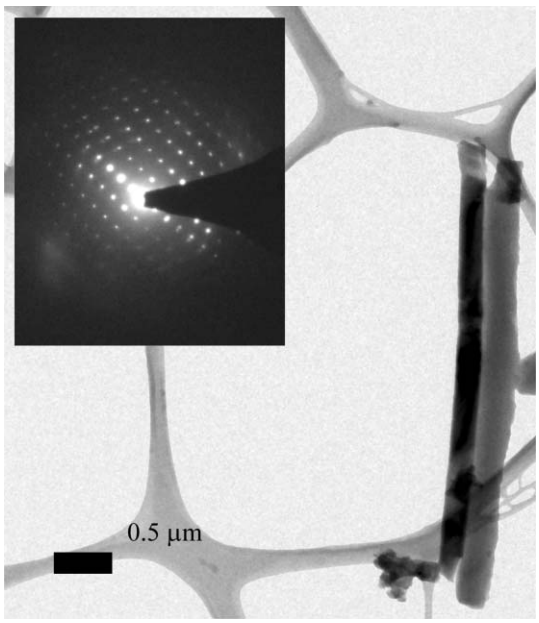


**Fig. 2** Dark field TEM image of DTBP nanorods. The darker nanorod is a single crystal (5 microns long and 200 nm thick). Inset: electron diffraction of the darker nanorod.

The two segments are almost completely uniform in color, one dark and one light. Since the presence of differently oriented crystal domains should show up as a speckled mix of dark and light regions in the image,[22] this image suggests that both rods consist almost entirely of single crystal domains. The act of depositing them on the graphite substrate leads to their random orientation with respect to each other. Closer inspection of the TEM image reveals regions where the crystal axis changes (near the top of the right hand rod, and near the bottom of the left hand rod) and the rod changes from dark to light or *vice versa*. These regions of crystal discontinuity probably result from twinning defects incurred when two separately growing crystal regions meet in the interior of the tube.[23] The inset to Fig. 2 shows the electron diffraction pattern from one of the rods. As expected, it exhibits a well-defined array of sharp spots, indicative of a single crystal rather than the rings which would be expected from a polycrystalline sample. Continued exposure of the rod to the electron beam caused it to become amorphous, at which point the electron diffraction pattern becomes a single uniform hue typical for amorphous solids.

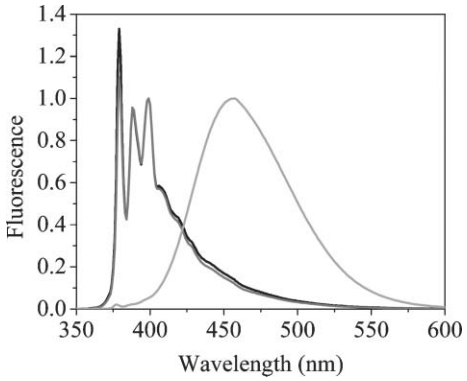


**Fig. 3** Normalized fluorescence spectra of DTBP. The spectra for DTBP bulk crystals (grey) and 200 nm nanorods (black) suspended in water overlap and are peaked at ~375 nm. The broad spectrum centered at ~450 nm corresponds to DTBP nanoparticles prepared by reprecipitation.

The optical properties of the DTBP nanorods are also consistent with its crystalline nature. Fig. 3 shows the fluorescence spectra of three different samples: a macroscopic single crystal of DTBP, the DTBP nanorods suspended in solution, and an aqueous suspension of DTBP nanoaggregates formed by the reprecipitation method. The spectra of the single crystal and the nanorods are nearly identical. The main discrepancy is the height of the short wavelength 0–0 vibronic peak, which is smaller in the macroscopic crystal. The decreased height of this peak is likely the result of self-absorption in the thicker crystal, relative to the much thinner nanorods. In addition, both the rod and the crystal spectra overlap well with the spectrum of monomeric DTBP in solution. This is because the crystal structure of solid DTBP does not permit the pi-stacking interactions that lead to excimer formation in unsubstituted pyrene.[24] Reprecipitation, on the other hand, leads to rapid aggregation and the formation of a disordered solid with pi-stacked aggregates. The broad, red-shifted emission from this sample is indicative of excimer formation and demonstrates the importance of growth conditions in obtaining well-defined spectroscopic behavior from these samples.

An important question is the mechanism of formation of the large crystalline domains in the Anodisc channels. To try to look at the intermediate structures in this process, we used 20 nm Anodisc filters. These smaller pore size filters actually consist of a 20 nm channel which extends a few microns into the filter, followed by a 200 nm channel which extends over the remainder of the 60 micron thickness of the Anodisc. We reasoned that the small diameter hole on one end would retard the entrance of solvent and solute into the channels and slow down rod formation. Fig. 4 shows the SEM

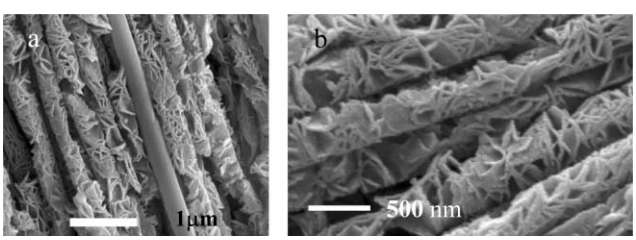


**Fig. 4** a) FESEM image of partially formed 200 nm DTBP nanorods. The platelets of DTBP crystals are ~ 20 nm thick. b) Close up view of the platelets.

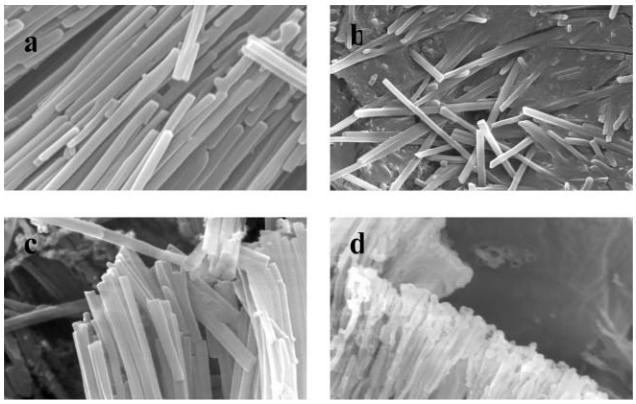


**Fig. 5** a) Cyanoanthracene nanorods (200 nm diameter). b) Tetra-*t*-butylperylene nanorods (200 nm). c) *m*-terphenyl nanorods (200 nm). d) *m*-terphenyl nanotubes.

image of these rods prepared under conditions identical to those of the rods seen in Fig. 1. The rods are composed of a jumble of platelets, roughly 20 nm thick, which extend across the channel diameter. We believe that the similarity of the platelet thickness and the end pore diameter is coincidental, since it is unlikely that the 20 nm pore could influence platelet thickness several microns away. Note also that although viewed from the side the platelets appear thin, several of them are turned so that their actual pancake-like shape can be discerned. From this image, it appears that the large single crystal domains seen in Fig. 2 are not the result of controlled growth from a single seed crystal, but rather the product of a continuous annealing process among many nanocrystals that proceeds over the course of hours. In our rods, the annealing process probably cannot eliminate mismatches between larger crystal regions, and when two such regions encounter each other, one expects to see the twinning defects apparent in Fig. 2. It is possible that extending the annealing period beyond 24 hours, or annealing at higher temperatures using a different solvent, could increase the size of the crystalline domains in Fig. 2.

The success of our efforts with DTBP led us to try this method with various other molecules. Fig. 5 shows rods composed of 9-cyanoanthracene, 2,5,8,11-tetra-*tert*-butylperylene, and *meta*-terphenyl. For comparison, Fig. 5d shows a sample made by simply immersing an Anodisc filter in a *meta*-terphenyl melt. For all these molecules, we found that the low-temperature solvent annealing method resulted in solid rods. Immersing the Anodisc in the melt, however, resulted in the tubular structures shown in Fig. 5d. These tubes also had a more irregular shape and were more susceptible to electron beam damage than the corresponding rods. For some other molecules, notably anthracene, pyrene, and perylene, we were unable to obtain high yields of rods using this method, although in the case of anthracene a mixture of rods and larger crystalline aggregates was obtained. We have not yet done a quantitative analysis of what molecular properties lead to successful rod formation, but two characteristics seem to have the greatest effect. First, the molecule must be highly soluble in the annealing solvent, at least at the temperature where the annealing is done. Not surprisingly, the addition of *tert*-butyl groups helps enable successful rod growth for pyrene and perylene. Second, the molecule must have a low vapor pressure at the annealing temperature so that sublimation does not compete with crystal growth. This is part of the difficulty with anthracene and pyrene, both of which are highly soluble, but which were also observed to sublime inside the preparation chamber. It should be emphasized that it may be possible to find a solvent/temperature combination which does produce high yields of rods for these compounds as well – our experiments so far have only used THF and $CH_2Cl_2$ as annealing solvents.

In conclusion, we have developed an inexpensive and rapid way to synthesize crystalline organic nanorods using low temperature solvent annealing and porous $Al_2O_3$ templates. The method works for a variety of conjugated organic compounds, and probably can be extended to many more by systematic variation of the solvent and temperature conditions. We are currently pursuing this, as well as trying to grow rods with much smaller diameters using custom-grown porous $Al_2O_3$ membranes. The ability to make single crystal, monodisperse organic nanorods should make it possible to systematically investigate phenomena like exciton confinement and size effects in well-defined, reproducible samples.

## Notes and references


1 T. Hasobe, P. V. Kamat, V. Troiani, N. Solladie, T. K. Ahn, S. K. Kim, D. Kim, A. Kongkanand, S. Kuwabata and S. Fukuzumi, *J. Phys. Chem. B*, 2005, **109**, 19.
2 B. S. Gaylord, S. Wang, A. J. Heeger and G. C. Bazan, *J. Am. Chem. Soc.*, 2001, **123**, 6417.
3 H. Kasai, H. S. Nalwa, H. Oikawa, S. Okada, H. Matsuda, N. Minami, A. Kakuta, K. Ono, A. Mukoh and H. Nakanishi, *Jpn. J. Appl. Phys.*, 1992, **31**, L1132.
4 H. B. Fu and J. N. Yao, *J. Am. Chem. Soc.*, 2001, **123**, 1434.
5 H. Kasai, H. Kamatani, S. Okada, H. Oidawa, H. Matsuda and H. Nakanishi, *Jpn. J. Appl. Phys.*, 1996, **35**, L221.
6 Z. Tian, Y. Chen, W. Yang, J. Yao, L. Zhu and Z. Shuai, *Angew. Chem., Int. Ed.*, 2004, **43**, 4060.
7 C. Martin, *Science*, 1994, **266**, 1961.
8 L. Zhi, J. Wu, J. Li, U. Kolb and K. Mullen, *Angew. Chem., Int. Ed.*, 2005, **44**, 2120.
9 L. Zhao, W. Yang, Y. Luo, T. Zhai, G. Zhang and J. Yao, *Chem.–Eur. J.*, 2005, **11**, 3773.
10 L. Zhao, W. Yang, Y. Ma, J. Yao, Y. Li and H. Liu, *Chem. Commun.*, 2003, 2442.
11 H. Gan, H. Liu, Y. Li, Y. Liu, F. Lu, T. Jiu and D. Zhu, *Chem. Phys. Lett.*, 2004, **399**, 130.
12 L. Qu and G. Shi, *Chem. Commun.*, 2004, 2800.
13 J. K. Lee, W. K. Koh, W. S. Chae and Y. R. Kim, *Chem. Commun.*, 2002, 138.
14 L. Zhi, T. Gorelik, J. Wu, U. Kolbe and K. Mullen, *J. Am. Chem. Soc.*, 2005, **127**, 12792.
15 M. Steinhart, J. H. Wendorff, A. Greiner, R. B. Wehrspohn, K. Nielsch, J. Schilling, J. Choi and U. Gosele, *Science*, 2002, **296**, 1997.
16 M. Steinhart, J. H. Wendorff and R. B. Wehrspohn, *ChemPhysChem*, 2003, **4**, 1171.
17 S. Loi, U. M. Wiesler, H. J. Butt and K. Mullen, *Chem. Commun.*, 2000, 1169.
18 H. Yanagi and T. Morikawa, *Appl. Phys. Lett.*, 1999, **75**, 187.
19 F. Balzer and H. G. Rubahn, *Surf. Sci.*, 2002, **507–510**, 588.
20 H. Liu, Y. Li, S. Xiao, H. Gan, T. Jiu, H. Li, L. Jiang, D. Zhu, D. Yu, B. Xiang and Y. Chen, *J. Am. Chem. Soc.*, 2003, **125**, 10794.
21 A. Miyazawa, T. Yamato and M. Tashiro, *Chem. Express*, 1990, **5**, 381.
22 G. Thomas and M. J. Goringe, *Transmission Electron Microscopy of Materials*; 1st edn; John Wiley & Sons: New York, 1979.
23 J. B. Wright, *Molecular Crystals*; 2nd edn; Cambridge University Press: Cambridge, UK, 1995.
24 A. C. Hazell and J. G. Lomborg, *Acta Crystallogr., Sect. B*, 1972, **28**, 1059.


 